

The influence of the dipolar forces on the static susceptibilities of Heisenberg ferromagnets

This article has been downloaded from IOPscience. Please scroll down to see the full text article.

1990 J. Phys.: Condens. Matter 2 7511

(<http://iopscience.iop.org/0953-8984/2/36/014>)

View [the table of contents for this issue](#), or go to the [journal homepage](#) for more

Download details:

IP Address: 171.66.16.151

The article was downloaded on 11/05/2010 at 06:53

Please note that [terms and conditions apply](#).

The influence of the dipolar forces on the static susceptibilities of Heisenberg ferromagnets

H S Toh and G A Gehring

Department of Theoretical Physics, Keble Road, Oxford OX1 3NP, UK

Received 23 March 1990, in final form 5 June 1990

Abstract. The longitudinal susceptibility of the Heisenberg ferromagnet, with short-range interactions only, is known to diverge below T_c at $H = 0$ as $1/k$ and at $k = 0$ as $H^{-1/2}$. This divergence has never been observed in neutron scattering experiments. We compute the longitudinal and transverse susceptibilities including dipolar effects at low temperatures and their variation with k and H . We use linear spin-wave theory and find that for $k^2 + H \ll m$, where m is the ratio of the dipolar strength to the exchange strength, the dipolar susceptibility is half that of the exchange-only susceptibility for both longitudinal and transverse cases. For $k^2 + H \gg m$, the two susceptibilities are asymptotically identical. Thus we conclude that it is the applied magnetic field that destroys the divergence. Numerical results are presented for the susceptibilities as a function of k and H .

1. Introduction

The properties of the longitudinal susceptibility χ^{zz} of ferromagnets with Heisenberg short-range interactions are surprisingly still the topic of controversy because the experimental situation is unclear [1]. Holstein and Primakoff [2] predicted that χ^{zz} diverges below T_c with the applied field h like $h^{-1/2}$. The calculations of Mazenko [3] found the wavevector dependence of χ^{zz} to diverge like $1/k$ in zero field. Brezin and Wallace [4] studied the longitudinal susceptibility of Heisenberg ferromagnets in the critical regime close to T_c and showed that it diverged in the critical regime with vanishing k and H as well. So far neutron scattering experiments have failed to detect any divergence for all temperatures below T_c .

Recently the longitudinal susceptibility $\chi^{zz}(k)$ has been measured using neutron scattering on EuO by Mitchell *et al* [5] and Ni by Mitchell and Mook [6] which are cubic ferromagnets with dipolar interactions. The experiments were performed at close to T_c with the scattering wavevector $k \geq 0.02\pi$ and the expected divergence was not observed. However a small field was applied to remove the domains caused by the dipolar interactions. According to the theories of Holstein [2] and Brezin [4], this applied field would be responsible for removing the divergence.

All real Heisenberg ferromagnets have a long-range dipolar interaction between the spins in addition to the short-range exchange interactions. It is, to our knowledge, undetermined how the dipolar forces affect the behaviour of χ^{zz} and its divergence in the low-temperature and low- k limit. Aharony and Bruce [7] have performed a renormalisation-group calculation for Heisenberg ferromagnets with dipolar interactions close to the transition temperature T_c . They found that the critical exponents

and scaling functions to be negligibly altered numerically when dipolar forces are included, and the longitudinal susceptibility still divergent in the critical regime below T_c with vanishing k and h .

This paper seeks to investigate the effects of dipolar interactions in the Heisenberg ferromagnets in the *low-temperature* regime. It seeks to determine, in the low-temperature regime, unambiguously the cause of the experimental failure to see the divergence. Using linear spin-wave theory, we calculate the longitudinal and transverse susceptibilities over the whole Brillouin zone while including dipolar effects, investigating their behaviour in the limit of vanishing k and magnetic field. Using the above results, we arrived at the conclusion that it was the magnetic field and not dipolar interactions that destroyed the divergence. What dipolar effects induce is a *halving* of the susceptibility when $(k^2 + h) \ll m$, where m is the dipolar field strength. For $(k^2 + h) \gg m$, the susceptibility is almost numerically the same as in the case without dipolar forces. We show that for the magnetic field strengths applied and range of k values measured in Mitchell and co-workers' experiments [5,6], the divergence would not be observed.

We have also computed the transverse susceptibilities $\chi^{+-}, \chi^{-+}, \chi^{--}, \chi^{++}$ using the same linear spin-wave theory, finding the transverse susceptibilities much more divergent in the small- k limit than the longitudinal susceptibility. To measure the longitudinal susceptibility experimentalists should use polarised scattering techniques to filter out the transverse susceptibilities. Again we found this halving effect in χ^{-+}, χ^{+-} due to dipolar forces as described for the longitudinal case. Without dipolar forces, $\chi^{--} = \chi^{++} = 0$ [8]. We found that for $k^2 + h \ll m$, $\chi^{--} = \chi^{++} \sim \frac{1}{2}\chi^{-+}$ (non-dipolar).

In section 2, using linear spin-wave approximations, we analytically derive the longitudinal and transverse susceptibilities of a three-dimensional Heisenberg ferromagnet with dipolar interactions for all values of k and h . In section 3, we present the analytical results for the asymptotic behaviour of the susceptibilities for the two limiting cases of small and large values of k and h respectively. The numerical results for all k and experimentally applied values of the field based on selected real crystals (EuO, Fe, Ni) are presented in section 4. In these calculations we have assumed that the longitudinal susceptibilities can be modelled by a Heisenberg model for the metallic ferromagnets Fe and Ni. Based on these numerical results, we concluded that Ni was likely to be the best candidate to measure the divergence of χ^{zz} .

2. Analytic derivation of the susceptibilities

We investigate $\chi^{zz}(k, h)$ in the low-temperature spin-wave regime as a function of the strength of the dipolar interactions, external field and temperature. Throughout this paper we consider only a simple cubic lattice.

The Hamiltonian for a ferromagnet with nearest-neighbour exchange energy of strength J and magnetic moment $M = g\mu_B S$ in a field \mathbf{B} applied in the z direction is given by

$$\mathcal{H}_0 = - \sum_{\langle ij \rangle} J \mathbf{S}_i \cdot \mathbf{S}_j - g\mu_B \sum_i B S_i^z - \frac{1}{2} \sum_{ij} \frac{(g\mu_B)^2}{|\mathbf{r}_i - \mathbf{r}_j|^5} \times \{3[\mathbf{S}_i \cdot (\mathbf{r}_i - \mathbf{r}_j)][\mathbf{S}_j \cdot (\mathbf{r}_i - \mathbf{r}_j)] - |\mathbf{r}_i - \mathbf{r}_j|^2 \mathbf{S}_i \cdot \mathbf{S}_j\}. \quad (1)$$

\mathbf{B} is the internal magnetic field, which takes into account the demagnetization field. The Hamiltonian should also include a magnetic anisotropy term, but for most high-symmetry cubic substances, including the ones this paper will touch on (EuO, Fe, Ni), its magnitude is very small compared with the exchange and dipolar energies (see section 4). We can represent this anisotropic term as an internal field incorporated into B .

Within the low-temperature linearised approximation, Holstein [2] obtained the Hamiltonian

$$\mathcal{H}_{\text{HP}} = C_1 - \frac{1}{2} \sum_q A_q + \sum_q \epsilon_q [c_q^\dagger c_q + \frac{1}{2}] \tag{2}$$

where the operators c_q and c_q^\dagger are given in terms of spin operators by

$$S_q^+ = \sqrt{2SN}(u_q c_q + v_q c_{-q}^\dagger) \tag{3a}$$

$$S_q^- = \sqrt{2SN}(u_q c_q^\dagger + v_q c_{-q}) \tag{3b}$$

$$u_q = u_{-q} = \sqrt{\frac{1}{2}} \sqrt{\frac{A_q}{\epsilon_q} + 1} \tag{4a}$$

$$v_q = v_{-q} = \sqrt{\frac{1}{2}} \sqrt{\frac{A_q}{\epsilon_q} - 1} \tag{4b}$$

$$\epsilon_q = \epsilon_{-q} = [A_q^2 - |B_q|^2]^{1/2} \tag{5a}$$

$$A_q = A_{-q} = 2JS(3 - \cos q_x - \cos q_y - \cos q_z) + 2SJh + 2SJm \sin^2 \theta_q \tag{5b}$$

$$B_q = B_{-q} = 2SJm \sin^2 \theta_q e^{2i\varphi} \tag{5c}$$

$$h = (g\mu_B B)/(2SJ). \tag{5d}$$

φ is the azimuthal angle of \mathbf{q} in the plane perpendicular to the z direction.

θ_q is the angle \mathbf{q} makes with the z direction. The wavevector \mathbf{q} is given in terms of radians. N is the number of spins per unit volume.

$$m = (2\pi(g\mu_B)^2 SN)/(2SJ)$$

m can be crudely thought of as the ratio of dipolar to exchange energies.

Having obtained this boson Hamiltonian, we can derive the susceptibilities. The details of the calculation are in the appendix.

The longitudinal susceptibility is

$$\begin{aligned} \chi^{zz}(\mathbf{k}, h) = (g\mu_B)^2 \sum_q & \left((u_q u_{q+k} + v_q v_{q+k})^2 \frac{n_q - n_{q+k}}{\epsilon_{q+k} - \epsilon_q} \right. \\ & \left. + 2(u_q u_{q+k} v_q v_{q+k} + u_q^2 v_{q+k}^2) \frac{n_q + n_{q+k} + 1}{\epsilon_q + \epsilon_{q+k}} \right) \end{aligned} \tag{6}$$

where $n_q = (e^{\beta\epsilon_q} - 1)^{-1}$ and $\beta = 1/k_B T$.

The transverse susceptibilities are

$$\chi^{+-}(\mathbf{k}, h) = \chi^{-+}(\mathbf{k}, h) = SN(g\mu_B)^2 \frac{u_k^2 + v_k^2}{\epsilon_k} \quad (7a)$$

$$\chi^{++}(\mathbf{k}, h) = \chi^{--}(\mathbf{k}, h) = 2SN(g\mu_B)^2 \frac{u_k v_k}{\epsilon_k}. \quad (7b)$$

By comparison, for the case of exchange interactions only,

$$m = 0 \Rightarrow v_k = B_k = 0$$

$$A_q(m = 0) = \epsilon_q(m = 0) \equiv \epsilon_q^0$$

$$\epsilon_q^0 = 2JS(3 - \cos q_x - \cos q_y - \cos q_z) + 2JS_h$$

$$n_q(m = 0) \equiv n_q^0 = (e^{\beta\epsilon_q^0} - 1)^{-1}$$

$$\chi_{\text{non-dipolar}}^{zz}(\mathbf{k}, h) = (g\mu_B)^2 \sum_q \frac{n_q^0 - n_{q+k}^0}{\epsilon_{q+k}^0 - \epsilon_q^0} \quad (8a)$$

$$\chi_{\text{non-dipolar}}^{-+}(\mathbf{k}, h) = \chi_{\text{non-dipolar}}^{+-}(\mathbf{k}, h) = SN \frac{(g\mu_B)^2}{\epsilon_k^0} \quad (8b)$$

$$\chi_{\text{non-dipolar}}^{--} = \chi_{\text{non-dipolar}}^{++} = 0.$$

We note that equation (7) differs from equation (9a) through the difference in the matrix elements as well as depending on the dipolar energies ϵ_q in place of non-dipolar energies ϵ_q^0 .

3. Asymptotic behaviour of susceptibilities

3.1. Longitudinal susceptibility

In this section we look at the low- k limit of the susceptibilities analytically so as to obtain physical insight into the results. χ^{zz} diverges in the limit of vanishing k and h , because most of the contribution to the integral expression of χ^{zz} comes from the region of small q . The integrand in the limit of vanishing q will be much larger than in the outer regions of the Brillouin zone. In this section we will work on the assumption that the dominant divergent contribution to the integrand as k and h go to zero will come from the infinitesimal region of vanishing q . This corresponds to small $\beta\epsilon_q$ (cf equation (6)). The predictions of this section will be subsequently justified by the numerical results of section 4. With that approximation we can expand in terms of $\beta\epsilon_q$ and the following functions can be approximated thus:

$$\frac{n_q - n_{q+k}}{\epsilon_{q+k} - \epsilon_q} \approx \frac{n_{q+k} + n_q + 1}{\epsilon_{q+k} + \epsilon_q} \approx \frac{1}{\beta} \frac{1}{\epsilon_{q+k}\epsilon_q}.$$

Then equation (6) becomes

$$\chi^{zz}(\mathbf{k}, h) \approx k_B T (g\mu_B)^2 \sum_q [(u_q u_{q+k} + v_q v_{q+k})^2 + 2(u_q u_{q+k} v_q v_{q+k} + u_q^2 v_{q+k}^2)] \frac{1}{\epsilon_{q+k}\epsilon_q}. \quad (9)$$

Using the relations (4) we find the following expression for the matrix element part of equation (9)

$$(u_q u_{q+k} + v_q v_{q+k})^2 + 2(u_q u_{q+k} v_q v_{q+k} + u_q^2 v_{q+k}^2) = \frac{A_q A_{q+k}}{\epsilon_{q+k} \epsilon_q} + \frac{|B_q B_{q+k}|}{\epsilon_{q+k} \epsilon_q} - \frac{A_q}{2\epsilon_q} + \frac{A_{q+k}}{2\epsilon_{q+k}}$$

and hence

$$\lim_{k \rightarrow 0} \chi^{zz}(\mathbf{k}, h) \approx k_B T (g\mu_B)^2 \sum_q \frac{A_q A_{q+k} + |B_q B_{q+k}|}{\epsilon_{q+k}^2 \epsilon_q^2}. \tag{10}$$

Equation (10) shows that $\chi^{zz}(\mathbf{k}, h)$ increases linearly with T , for small k . However it is actually a good approximation for the whole Brillouin zone as can be seen from figure 8.

Using the form of A_q, ϵ_q given in equations (5a), (5b), it can be shown that

$$\begin{aligned} \lim_{k \rightarrow 0} \chi^{zz}(\mathbf{k}, h) &= \frac{k_B T}{2(2SJ)^2} (g\mu_B)^2 \sum_q \frac{1}{[q^2 + h][|q + k|^2 + h]} \\ &+ \frac{k_B T}{2(2SJ)^2} (g\mu_B)^2 \sum_q \frac{1}{[q^2 + h + 2m \sin^2 \theta_q][|q + k|^2 + h + 2m \sin^2 \theta_{q+k}]} \end{aligned}$$

When the dipolar forces are absent, $m = 0$, and we obtain the standard result for the non-dipolar case which can be obtained from equation (8a) (cf [2, 3])

$$\begin{aligned} \chi_{\text{non-dipolar}}^{zz}(\mathbf{k}, h) &= \frac{k_B T}{(2SJ)^2} (g\mu_B)^2 \sum_q \frac{1}{[q^2 + h][|q + k|^2 + h]} \\ &\sim \frac{1}{k} \quad h = 0, k \rightarrow 0 \\ &\sim \frac{1}{\sqrt{h}} \quad k = 0, h \rightarrow 0. \end{aligned}$$

We can write

$$\chi_{\text{dipolar}}^{zz}(\mathbf{k}, h) = \frac{1}{2} \chi_{\text{non-dipolar}}^{zz}(\mathbf{k}, h) + I_0(\mathbf{k}, h). \tag{11}$$

When $k^2 + h \gg m$, B_q, B_{q+k} can be neglected, and

$$\begin{aligned} I_0(\mathbf{k}, H) &\sim \frac{k_B T}{2(2SJ)^2} (g\mu_B)^2 \sum_q \frac{1}{[q^2 + h][|q + k|^2 + h]} \\ &\sim \frac{1}{2} \chi_{\text{non-dipolar}}^{zz}. \end{aligned} \tag{12}$$

In this regime,

$$\chi_{\text{dipolar}}^{zz} = \chi_{\text{non-dipolar}}^{zz}$$

as expected.

We now examine the case where $k^2 + h \ll m$. $\chi_{\text{non-dipolar}}^{zz}$ diverges for small h, k . Setting $k = h = 0$, it can be shown that

$$\begin{aligned} I_0(0,0) &\propto \int \int \frac{q^2 dq \sin \theta d\theta}{[q^2 + 2m \sin^2 \theta]^2} \\ &\approx \int \int \frac{q^2 dq \theta d\theta}{[q^2 + 2m\theta^2]^2} \\ &\approx - \int q^2 dq \left(\frac{1}{4mq^2} + \text{constant} \right) \end{aligned} \quad (13)$$

is finite—in other words, $I_0(\mathbf{k}, h)$ is non-divergent in this limit of vanishing k, h .

I_0 can then be neglected, and

$$\chi_{\text{dipolar}}^{zz} = \frac{1}{2} \chi_{\text{non-dipolar}}^{zz} \quad (14)$$

in the dipolar limit $k^2 + h \ll m$. The dipolar susceptibility in this limit is essentially the non-dipolar susceptibility, except that its magnitude is *halved*. The dipolar susceptibility is thus isotropic like the non-dipolar case, even though dipolar forces are anisotropic. All the angular directional dependence of \mathbf{k} is contained in the non-divergent term $I_0(\mathbf{k}, h)$, so the asymptotic behaviour of χ^{zz} for $k^2 + h \ll m$ is independent of direction. For $k^2 + h \gg m$, $\chi^{zz} \sim \chi_{\text{non-dipolar}}^{zz}$, which is isotropic. Thus, over the whole Brillouin zone, χ^{zz} is almost independent of the direction of \mathbf{k} . This is confirmed by our numerical calculations.

We can also explain this ‘splitting off’ of the dipolar susceptibility into an isotropic divergent part and an anisotropic non-divergent part in terms of the transverse susceptibilities in section 3.3.

3.2. Transverse susceptibilities

We now examine the behaviour of the transverse susceptibilities. It can be shown using equations (4), (5) and (7) that

$$\chi^{-+}(\mathbf{k}, h) = \chi^{+-}(\mathbf{k}, h) = (g\mu_B)^2 S N A_k / \epsilon_k^2 \quad (15a)$$

$$\chi^{--}(\mathbf{k}, h) = \chi^{++}(\mathbf{k}, h) = (g\mu_B)^2 S N B_k / \epsilon_k^2. \quad (15b)$$

Using explicit forms of A_k, B_k, ϵ_k and m ,

$$\chi^{-+}(\mathbf{k}, h) = \chi^{+-}(\mathbf{k}, h) = \frac{m}{4\pi} \left(\frac{1}{2(k^2 + h)} + \frac{1}{2(k^2 + h + 2m \sin^2 \theta_k)} \right) \quad (16a)$$

$$\chi^{--}(\mathbf{k}, h) = \chi^{++}(\mathbf{k}, h) = \frac{m}{4\pi} \left(\frac{1}{2(k^2 + h)} - \frac{1}{2(k^2 + h + 2m \sin^2 \theta_k)} \right). \quad (16b)$$

Note the explicit dependence of the transverse susceptibilities on the direction of \mathbf{k} , introduced by dipolar forces, whereas the longitudinal susceptibility is essentially isotropic.

In the dipolar limit $k^2 + h \ll 2m$, this angular dependence causes the transverse susceptibilities to behave differently in the region of small θ_k and large θ_k .

For large values of θ_k such that $k^2 + h \ll 2m \sin^2 \theta_k$,

$$\chi^{++}(\mathbf{k}, h) = \chi^{--}(\mathbf{k}, h) = \chi^{+-}(\mathbf{k}, h) = \chi^{-+}(\mathbf{k}, h) = \frac{m}{(4\pi)} \frac{1}{2(k^2 + h)}.$$

For small values of θ_k such that $k^2 + h \gg 2m \sin^2 \theta_k$ and for all values of θ when $k^2 + h \gg 2m$,

$$\begin{aligned} \chi^{-+}(\mathbf{k}, h) &= \chi^{+-}(\mathbf{k}, h) = \frac{m}{4\pi} \frac{1}{k^2 + h} \\ \chi^{--}(\mathbf{k}, h) &= \chi^{++}(\mathbf{k}, h) \sim 0 \end{aligned}$$

which is the non-dipolar result.

We see a halving effect in χ^{-+} similar to χ^{zz} brought about by dipolar forces. Dipolar forces cause χ^{--} to diverge rapidly for $k^2 + h \ll 2m \sin^2 \theta_k$; without dipolar forces $\chi^{--} = \chi^{++} = 0$ throughout the whole Brillouin zone. For dipolar ferromagnets, as k and h go to zero, all transverse susceptibilities diverge much more strongly than the longitudinal susceptibility, approximately like the square of the longitudinal susceptibility.

Note that within the approximations of linear spin-wave theory, which is restricted to low temperatures, the transverse susceptibilities are independent of temperature.

3.3. Longitudinal susceptibility revisited

We can relate the asymptotic behaviour of the longitudinal susceptibility to that of the transverse susceptibilities. In the integral expression for χ^{zz} (equation (6)), the dominant contribution to the integrand comes from the limit of vanishing q . This is true for all values of k and h . Thus we can apply the approximate expression for χ^{zz} for all values of k and h from equation (10).

Using the expression for the transverse susceptibilities from equation (15):

$$\chi^{zz}(\mathbf{k}, h) \approx k_B T \left(\frac{1}{g\mu_B SN} \right)^2 \sum_q [\chi_q^{-+} \chi_{q+k}^{-+} + \chi_q^{--} \chi_{q+k}^{++}]. \quad (17)$$

We define

$$\chi_{\text{non-dipolar}}^{-+}(k) \equiv \frac{m}{4\pi} \frac{1}{k^2 + h}$$

and

$$U(\theta_k) \equiv \frac{m}{4\pi} \frac{1}{k^2 + h + 2m \sin^2 \theta_k}.$$

Using equation (16), we can then write

$$\chi^{zz}(k, h) \approx k_B T \left(\frac{1}{g\mu_B SN} \right)^2 \sum_q \left[\frac{1}{2} \chi_{\text{non-dipolar}}^{-+}(q) \chi_{\text{non-dipolar}}^{-+}(q+k) + \frac{1}{2} U(\theta_q) U(\theta_{q+k}) \right]. \quad (18)$$

Note that $\sum_q U(\theta_q) U(\theta_{q+k})$ is nothing more than $I_0(k, h)$ (cf equation (11)).

4. Numerical results

We have numerically integrated equations (7), (8) over the whole Brillouin zone to demonstrate the asymptotic behaviour predicted in section 3. We determine $2SJ$ in terms of T_c , using the approximate mean-field relation:

$$2SJ = \frac{3k_B T_c}{z(S+1)}$$

where z is the number of nearest neighbours.

We have plotted the susceptibilities of the real compounds, EuO, Fe and Ni, in the hope that experimentalists will compare with our numbers. EuO is a ferromagnetic insulator and is well described by the Hamiltonian in equation (1). Fe, Ni are both conducting metals and itinerant magnets. We use the model of a Heisenberg ferromagnet described in equation (1) as an approximate description of them, because we know that low-frequency spin-wave modes are observed in the metals. The data used to represent the magnets EuO, Fe and Ni are given in table 1.

Table 1. Data used to represent the magnets EuO, Fe and Ni.

| Fe | Ni | EuO |
|---|---|---|
| $k_D = 0.13$ | $k_D = 0.045$ | $k_D = 0.38$ |
| $T_c = 1040$ K | $T_c = 631$ K | $T_c = 69$ K |
| $S = 1$ | $S = 1/2$ | $S = 7/2$ |
| $z = 8$ | $z = 12$ | $z = 6$ |
| $N = 8.5 \times 10^{22}$ cm ⁻³ | $N = 9.2 \times 10^{22}$ cm ⁻³ | $N = 2 \times 10^{22}$ cm ⁻³ |

Notation. Following Mezei [9], we have defined the dipolar wavevector $k_D = \sqrt{m} = \sqrt{\pi N/Jg\mu_B}$. One can think of k_D as the magnitude of the wavevector at which the crossover between the dipolar and non-dipolar regimes occur.

We define W to be the anisotropy energy. The ratio of the anisotropy to exchange energies is

$$\frac{W}{J} = \begin{cases} O(10^{-3}) & \text{for Fe (cf [10])} \\ O(10^{-4}) & \text{for Ni (cf [11])} \end{cases}$$

m is roughly the ratio of dipolar to exchange energies. Comparing W/J to

$$m = \begin{cases} 0.017 & \text{for Fe} \\ 0.002 & \text{for Ni} \end{cases}$$

we can see that the anisotropy energy is negligible not only to the exchange but the dipolar energy as well.

Numerical results are computed for the following quantities.

A. Longitudinal susceptibility as a function of magnetic field of the following crystals compared with the non-dipolar longitudinal susceptibility without a field: EuO, Fe, Ni, at $T = \frac{1}{2}T_c$.

B. Transverse susceptibilities χ^{++} , χ^{+-} in the absence of a field for the following crystals compared with the non-dipolar transverse susceptibility χ^{+-} : EuO, Fe, Ni.

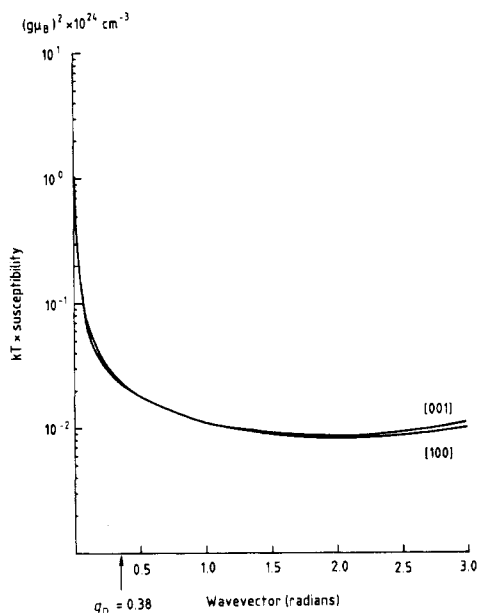


Figure 1. $k_B T \chi^{zz}$ of EuO along the transverse direction ($k00$) and the z direction ($00k$). $T = T_c/2$ and $h = 0$. This graph demonstrates that χ^{zz} is almost independent of the direction of \mathbf{k} throughout the Brillouin zone.

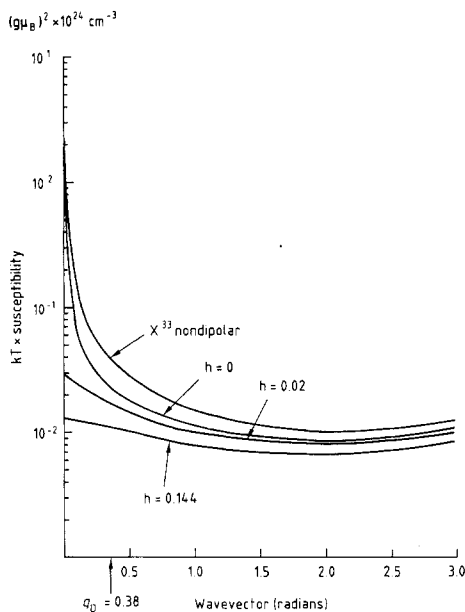


Figure 2. $k_B T \chi^{zz}$ of EuO as a function of k at $T = T_c/2$, with $h = 0$, $h = 0.02$, $h = m$. $\chi_{\text{non-dipolar}}^{zz}$ of EuO is also plotted for comparison. $S = 7/2$ for all susceptibilities.

EuO is a simple cubic crystal, and Fe and Ni have bcc and fcc symmetry respectively. In our numerical integration programme we have assumed a simple cubic Brillouin zone of edge 2π , and wavevectors q, k are in units of radians. Our asymptotic analysis of section 3 has shown χ^{zz} to be almost independent of the direction of \mathbf{k} , as numerically demonstrated by figure 1. Therefore, in all other figures showing χ^z , we have taken \mathbf{k} to be along the z direction ($\{001\}$).

As shown in section 3, the transverse susceptibilities are highly dependent on the direction of \mathbf{k} . If $\theta_k = 0$, i.e. $\mathbf{k} = (0, 0, k)$, the transverse susceptibilities will be those for the non-dipolar case and there will be no dipolar crossover effects. In our figures, we have chosen $\mathbf{k} = (k, 0, 0)$, i.e. $\sin^2 \theta_k = 1$ and the dipolar crossover behaviour of $\chi^{++} = \chi^{--}$ is highly visible. By symmetry, $(k, 0, 0)$ and $(0, k, 0)$ are equivalent as far as the transverse susceptibilities are concerned.

The values of the dipolar strength m are taken from [5, 6, 9]. Mitchell and co-workers [5, 6] applied an external magnetic field of 0.1 T to EuO and 0.8 T to Ni. The internal field seen by the magnetic spins will be smaller than these external field strengths due to demagnetization effects; nevertheless, we have chosen to plot for these values of the applied field. Using the formula $h = (z(S+1)g\mu_B B)/(3k_B T_c)$, this translates to $h = 0.02$ for EuO and $h = 0.1$ for Ni. We have also plotted the case of $h = m$ for Fe and EuO with the crudely approximate assumption that that is the applied field strength required to remove domains created by dipolar interactions. The data in the following figures were obtained by numerical integration of equations (7) and (8). Mitchell and co-workers [5, 6] performed experimental measurements close to T_c , at about $0.9T_c$. In this regime the assumptions used in the low-temperature linear

spin-wave theory in this paper would break down; nonlinear interacting terms become important, rendering the calculation extremely difficult. At temperatures much closer to T_c , e.g. in the range $0.99T_c - T_c$, the renormalisation-group methods of Aharony and Bruce [7] would be appropriate. To preserve the validity of our calculations, we have chosen to compute our numerical results for eratures no higher than $T_c/2$.

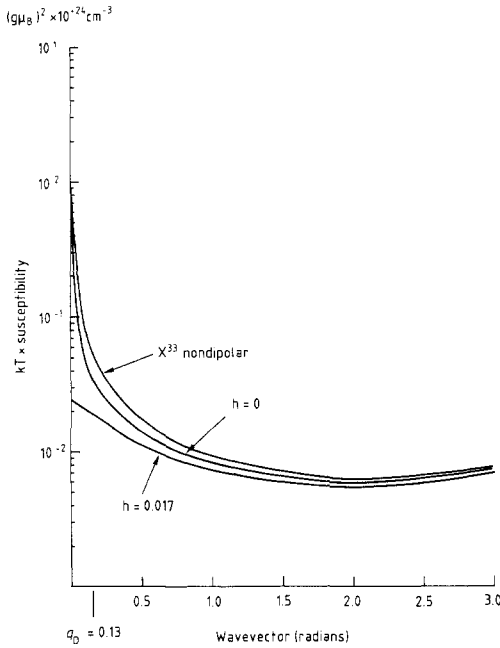


Figure 3. $k_B T \chi^{zz}$ of Fe as a function of k at $T = T_c/2$ with $h = 0$, $h = m$. $\chi_{\text{non-dipolar}}^{zz}$ of Fe is also plotted for comparison. $S = 1$ for all susceptibilities.

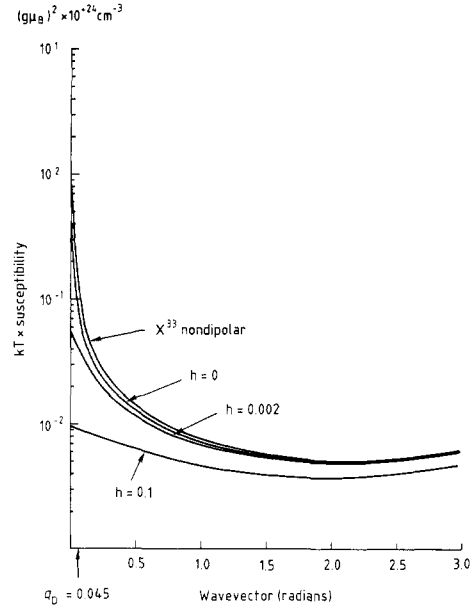


Figure 4. $k_B T \chi^{zz}$ of Ni as a function of k at $T = T_c/2$ with $h = 0$, $h = 0.1$, $h = m$. $\chi_{\text{non-dipolar}}^{zz}$ of Ni is also plotted for comparison. $S = 1/2$ for all susceptibilities.

Because k_D is so small for all three magnets, the figures for χ^{zz} do not demonstrate the crossover to the dipolar regime very well. To demonstrate the predicted halving effect due to dipolar effects clearly, table 2 shows the numerical data for the longitudinal susceptibility of EuO.

The susceptibilities are in units of $(g\mu_B)^2 \times 10^{24} \text{ cm}^{-3}$. $h = 0$, $T = T_c/2$. Observe that for $k_z < k_D$, χ^{zz} is about half $\chi_{\text{non-dipolar}}^{zz}$. For $k_z \gg k_D$, the two susceptibilities are roughly equal. The numerical data indicate that a divergence will be detected at $k_z \leq 0.1$. However, we must remember that in this case $h = 0$, and that even a small value of h will reduce the divergence at small k_z , as the figures indicate.

From the figures we can see that in order to detect any of the predicted divergence even in the absence of a field, measurements must be taken with the magnitude of the scattering wavevector k smaller than 0.01 rad. For k larger than 0.01 the longitudinal susceptibility is relatively flat. The experiments performed by Cowley and Mitchell [1] and Mitchell and co-workers [5, 6] measured at wavevectors no smaller than 0.01 rad. Experiments measuring χ^{zz} must be done on single-domain crystals. Dipolar forces cause multiple domains to form, and a magnetic field needs to be applied to remove domains. The figures show that even a small magnetic field will reduce the divergence by several orders of magnitude. The larger the dipolar strength m , the stronger the

Table 2. Numerical data for the longitudinal susceptibility of EuO.

| k_z | $k_B T \chi_{\text{non-dipolar}}^{zz}$ | $k_B T \chi^{zz}$ |
|-------------------|--|-------------------|
| 0.001 | 13.0 | 6.48 |
| 0.01 | 1.31 | 0.635 |
| 0.1 | 0.13 | 0.064 |
| 0.2 | 0.067 | 0.035 |
| 0.3 | 0.045 | 0.026 |
| 0.4 $\approx k_D$ | 0.034 | 0.021 |
| 0.5 | 0.028 | 0.018 |
| 0.6 | 0.0236 | 0.016 |
| 0.8 | 0.018 | 0.013 |
| 1.0 | 0.015 | 0.011 |
| 2.0 | 0.010 | 0.0085 |
| 3.0 | 0.0125 | 0.011 |

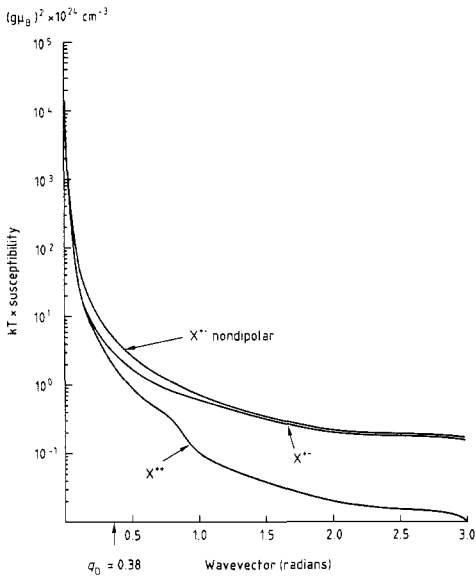


Figure 5. Transverse susceptibilities of EuO. $k_B T \chi^{++} = k_B T \chi^{--}$, $k_B T \chi^{-+} = k_B T \chi^{+-}$ are plotted. The sharp decay of χ^{--} after k_D most visibly demonstrates the dipolar crossover effect. $k_B T \chi_{\text{non-dipolar}}^{-+} = k_B T \chi_{\text{non-dipolar}}^{+-}$ is also plotted for comparison. $h = 0$ and \mathbf{k} is along the x direction. By symmetry, \mathbf{k} along the y direction would have produced the same result. $T = T_c/2$.

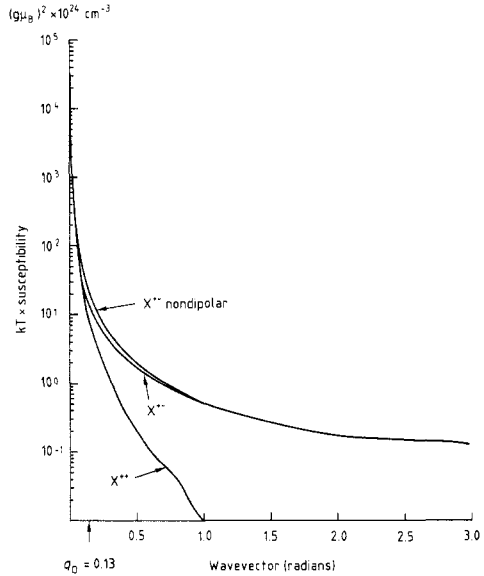


Figure 6. $k_B T \times$ transverse susceptibilities of Fe. $h = 0$, $T = T_c/2$.

magnetic field h is required. It appears that Ni, based on the approximate model of a Heisenberg ferromagnet in equation (1), with the smallest dipolar strength m , is the best candidate to experimentally detect divergent behaviour. The temperature in relation to the Curie temperature T_c , will affect the longitudinal susceptibility χ^{zz} ; this can be deduced by comparing the figures of χ^{zz} at $T = T_c/2$ with those at $T = T_c/4$. χ^{zz} varies with T in a quasilinear way. The lower the temperature, the smaller the value of χ^{zz} . Within the framework of low-temperature spin-wave theory,

we found the transverse susceptibilities independent of temperature. The transverse susceptibilities show the most obvious indication of a crossover from the dipolar to non-dipolar behaviour, particularly the rapid decay of $\chi^{++} (= \chi^{--})$ after the dipolar wavevector k_D .

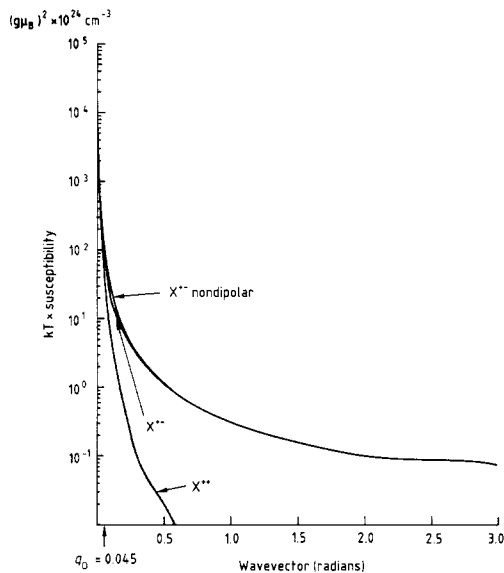


Figure 7. $k_B T \times$ transverse susceptibilities of Ni. $h = 0$, $T = T_c/2$.

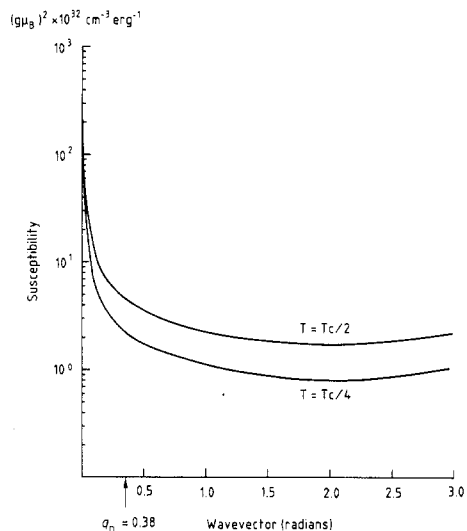


Figure 8. Longitudinal susceptibility χ^{zz} of EuO for $T = T_c/2$ and $T = T_c/4$. $h = 0$. This is to demonstrate the temperature dependence of χ^{zz} . We can generalise this temperature dependence to all cases of longitudinal susceptibility with various values of h and m , of various real substances.

The transverse susceptibility χ^{-+} appears about an order of magnitude larger than the longitudinal. This is partly due to the much faster divergence of the transverse susceptibilities in the low- k region.

Neutron scattering experiments do not measure χ directly, but the scattering cross section $d^2\sigma/d\Omega dE$ which is proportional to $k_B T \chi$. Thus we choose to plot $k_B T \chi$ instead of χ for all diagrams except figure 8. $k_B T \chi$ is temperature dependent in both the longitudinal and transverse cases, whereas χ is temperature dependent only in the longitudinal case. Since the purpose of figure 8 is to demonstrate the temperature dependence of the longitudinal susceptibility χ^{zz} , χ^{zz} instead of $k_B T \chi^{zz}$ is plotted for figure 8.

5. Conclusion

Holstein and Primakoff [2] showed that in the low-temperature regime, for zero k , the longitudinal susceptibility diverged as $h^{-1/2}$. Mazenko [3] found the longitudinal susceptibility to diverge in zero magnetic field as $1/k$. To our knowledge so far no experiment has confirmed the above predictions. Neither results took dipolar effects

into account. We have included the effects of dipolar interactions and shown that the power law nature of the divergences of the longitudinal susceptibility with k and h is unchanged. What the dipolar interactions effect is a *halving* of the magnitude of the longitudinal susceptibility for $(k^2 + h) \ll m$. The factor that destroys the divergence of the longitudinal susceptibility is the applied magnetic field, as originally predicted by Holstein. Even in the absence of a field, our figures indicate that experiments need to be conducted at $k < 0.01$ to detect this divergence. Numerical curves have been obtained for the various susceptibilities as a function of magnetic field strength h over the whole Brillouin zone. Our numerical results indicate that Ni, with the smallest dipolar strength m and hence requiring a smaller magnetic field to remove domains created by dipolar interaction, would be the best candidate to detect any divergence.

We have also analytically calculated the behaviour of the transverse susceptibilities including dipolar effects and found that, as for the longitudinal case, dipolar effects *halve* the susceptibilities for $(k^2 + h) \ll 2m \sin^2 \theta_k$. Unlike the longitudinal case, the transverse susceptibilities with dipolar interactions are highly dependent on the direction of the scattering wavevector. The other important difference is that the transverse susceptibilities are independent of temperature within the framework of our analytical approximations. We show that the halving effect of the longitudinal susceptibility can be related to the halving effect of the transverse susceptibilities.

Acknowledgments

We wish to thank Professor Cowley for the advice and references he provided for this paper, and Professor V Baryakhtar for comments on the manuscript.

Appendix. Longitudinal susceptibility

We apply a small spatially sinusoidal field in the z direction:

$$h_z(r) = h'(e^{ikr} + e^{-ikr}) \quad (\text{A1a})$$

$$\Rightarrow h_z(q) = h'N(\delta_{q+k} + \delta_{q-k}) \quad (\text{A1b})$$

At low temperatures, the system is near saturation, so we can approximate

$$\begin{aligned} S^z(r) &= S - \left(\frac{1}{2S}\right) S^-(r)S^+(r) \\ \Rightarrow S^z(k) &= NS\delta_k - \left(\frac{1}{2SN}\right) \sum_q S^-(q)S^+(q+k) \\ &= -\left(\frac{1}{2SN}\right) \sum_q S^-(q)S^+(q+k) \quad k \neq 0 \\ &= -\sum_q [u_q u_{q+k} c_q^\dagger c_{q+k} + v_q v_{q+k} c_{-q} c_{-q-k}^\dagger + u_q v_{q+k} c_q^\dagger c_{-q-k}^\dagger + v_q u_{q+k} c_{-q} c_{q+k}]. \end{aligned} \quad (\text{A2})$$

We used the expressions for S^- , S^+ from section 2 to obtain the expression for S^z in terms of the bosonic operators c, c^\dagger .

To \mathcal{H}_{HP} we add

$$g\mu_B \sum_r h_z(r) S^z(r) = -g\mu_B \frac{h'}{2SN} \sum_q [S^-(q)S^+(q+k) + S^-(q)S^+(q-k)].$$

The new Hamiltonian is

$$\mathcal{H}_z = \mathcal{H}_{\text{HP}} - g\mu_B \frac{h'}{2SN} \sum_q [S^-(q)S^+(q+k) + S^-(q)S^+(q-k)]. \quad (\text{A3})$$

\mathcal{H}_z is then expressed in terms of c, c^\dagger .

The equations of motions are

$$i\hbar \frac{d}{dt} c_q^\dagger(t) = [c_q^\dagger, \mathcal{H}_z] \quad (\text{A4a})$$

$$i\hbar \frac{d}{dt} c_q(t) = [c_q, \mathcal{H}_z]. \quad (\text{A4b})$$

Since h' is small, the equations of motion are linearised to first order in h' , from which the linearised solutions are obtained:

$$\begin{aligned} c_q^\dagger(t) = & e^{i\epsilon_q t/\hbar} c_q^\dagger + g\mu_B h' \left((u_{q-k}u_q + v_q v_{q-k}) \frac{\exp[(it/\hbar)\epsilon_{q-k}]}{\epsilon_{q-k} - \epsilon_q} c_{q-k}^\dagger \right. \\ & + (u_q u_{q+k} + v_q v_{q+k}) \frac{\exp[(it/\hbar)\epsilon_{q+k}]}{\epsilon_{q+k} - \epsilon_q} c_{q+k}^\dagger \\ & - (v_q u_{q-k} + v_{q-k} u_q) \frac{\exp[-(it/\hbar)\epsilon_{q-k}]}{\epsilon_{q-k} + \epsilon_q} c_{q-k} \\ & \left. - (v_q u_{q+k} + v_{q+k} u_q) \frac{\exp[-(it/\hbar)\epsilon_{q+k}]}{\epsilon_{q+k} + \epsilon_q} c_{-q-k} \right) \end{aligned} \quad (\text{A5})$$

and similarly for $c_q(t)$.

To first order,

$$-g\mu_B \langle S^z(k, t) \rangle = \chi^{zz}(k) h'. \quad (\text{A6})$$

We express $S^z(k, t)$ in terms of $c_k(t), c_k^\dagger(t)$, which in turn can be expressed in terms of c_k, c_k^\dagger , then take thermal averages and apply the thermal relations.

$$\begin{aligned} \langle S^z(k, t) \rangle = & -g\mu_B h' \sum_q \left((u_q u_{q+k} + v_q v_{q+k})^2 \frac{n_q - n_{q+k}}{\epsilon_{q+k} - \epsilon_q} \right. \\ & \left. + 2(u_q u_{q+k} v_q v_{q+k} + u_q^2 v_{q+k}^2) \frac{n_{q+k} + n_q + 1}{\epsilon_{q+k} + \epsilon_q} \right). \end{aligned} \quad (\text{A7})$$

All time-dependent terms cancel out. Thus, we obtain

$$\chi^{zz}(k) = (g\mu_B)^2 \sum_q \left((u_q u_{q+k} + v_q v_{q+k})^2 \frac{n_q - n_{q+k}}{\epsilon_{q+k} - \epsilon_q} + 2(u_q u_{q+k} v_q v_{q+k} + u_q^2 v_{q+k}^2) \frac{n_{q+k} + n_q + 1}{\epsilon_{q+k} + \epsilon_q} \right). \quad (\text{A8})$$

Note added in proof. We have just uncovered a paper (Pokrovsky V L 1979 *Adv. Phys.* **28**) in which the author predicted analytically the halving effect in the susceptibilities due to dipolar interactions. He also addressed the question as to why the $\hbar^{-1/2}$ divergence had not been seen by experimentalists so far; like us, he stated that in principle the divergence could be seen, but there are all sorts of technical difficulties involved in the experimental measurements.

References

- [1] Cowley R A and Mitchell X Y 1985 unpublished
- [2] Holstein T and Primakoff H 1940 *Phys. Rev.* **58** 1098
- [3] Mazenko G 1976 *Phys. Rev. B* **14** 3933
- [4] Brezin E, Wallace D J and Wilson K G 1973 *Phys. Rev. B* **7** 232
- [5] Mitchell P W, Hewitt M A and Mook H A 1989 unpublished
- [6] Mitchell P W and Mook H A 1988 unpublished
- [7] Aharony A and Bruce A 1974 *Phys. Rev. B* **7** 2973
- [8] Marshall W and Lovesey S W 1971 *Theory of Thermal Neutron Scattering* (Oxford: Oxford University Press)
- [9] Mezei F 1986 *Physica B* **136** 417
- [10] Kittel C 1986 *Introduction to Solid State Physics* (New York: Wiley)
- [11] Bleaney B I and Bleaney B 1985 *Electricity and Magnetism* (Oxford: Oxford University Press)